Synthetic and Systems Biotechnology 9 (2024) 115–126

Contents lists available at ScienceDirect

Synthetic and Systems Biotechnology

journal homepage: www.keaipublishing.com/en/journals/synthetic-and-systems-biotechnology

Original Research Article

Regulatory mechanisms of dopamine metabolism in a marine *Meyerozyma guilliermondii* GXDK6 under NaCl stress as revealed by integrative multi-omics analysis

Huijie Sun [a,b], Huashan Bai [a], Yonghong Hu [d], Sheng He [c], Ruihang Wei [a], Duotao Meng [a], Qiong Jiang [a], Hongping Pan [a], Peihong Shen [a], Qian Ou [a], Chengjian Jiang [a,b,*]

[a] State Key Laboratory for Conservation and Utilization of Subtropical Agro-bioresources, Guangxi Research Center for Microbial and Enzyme Engineering Technology, College of Life Science and Technology, Guangxi University, Nanning, 530004, China
[b] Guangxi Key Laboratory for Green Processing of Sugar Resources, College of Biological and Chemical Engineering, Guangxi University of Science and Technology, Liuzhou, 545006, China
[c] Guangxi Key Laboratory of Birth Defects Research and Prevention, Guangxi Key Laboratory of Reproductive Health and Birth Defect Prevention, Guangxi Zhuang Autonomous Region Women and Children Health Care Hospital, Nanning, 530033, China
[d] College of Food Science and Light Industry, Nanjing Tech University, No. 30, South Puzhu Road, Nanjing, 211816, China

ARTICLE INFO

Keywords:
Dopamine biosynthesis
Multi-omics analysis
NaCl stress
Meyerozyma guilliermondii

ABSTRACT

Dopamine can be used to treat depression, myocardial infarction, and other diseases. However, few reports are available on the de novo microbial synthesis of dopamine from low-cost substrate. In this study, integrated omics technology was used to explore the dopamine metabolism of a novel marine multi-stress-tolerant aromatic yeast *Meyerozyma guilliermondii* GXDK6. GXDK6 was found to have the ability to biosynthesize dopamine when using glucose as the substrate. 14 key genes for the biosynthesis of dopamine were identified by whole genome-wide analysis. Transcriptomic and proteomic data showed that the expression levels of gene *AAT2* encoding aspartate aminotransferase (regulating dopamine anabolism) were upregulated, while gene *AO-I* encoding copper amine oxidase (involved in dopamine catabolism) were downregulated under 10 % NaCl stress compared with non-NaCl stress, thereby contributing to biosynthesis of dopamine. Further, the amount of dopamine under 10 % NaCl stress was 2.51-fold higher than that of zero NaCl, which was consistent with the multi-omics results. Real-time fluorescence quantitative PCR (RT-qPCR) and high-performance liquid chromatography (HPLC) results confirmed the metabolic model of dopamine. Furthermore, by overexpressing *AAT2*, AST enzyme activity was increased by 24.89 %, the expression of genes related to dopamine metabolism was enhanced, and dopamine production was increased by 56.36 % in recombinant GXDK6AAT2. In conclusion, *Meyerozyma guilliermondii* GXDK6 could utilize low-cost carbon source to synthesize dopamine, and NaCl stress promoted the biosynthesis of dopamine.

1. Introduction

As a neurotransmitter transmits signals in the brain, dopamine can change in its level to affect people's behavior, such as learning memory, exercise, and emotion [1]. Insufficient production amounts of dopamine can cause Parkinson's disease, schizophrenia, and heart diseases in humans [2]. Dopamine is effective in the treatment of depression, myocardial infarction, and other diseases [3]. At present, dopamine can be synthesized from the frontal cortex and striatum of the animal brain, such as rats [4]. In addition, dopamine can be produced in plant organs [5]. Dopamine inhibits plant senescence and influences nutrient concentrations under drought conditions by regulating the uptake, transport, and resorption of nutrients [6]. Furthermore, the chemical synthesis of dopamine has the problems of high production cost, low conversion efficiency, high requirements for equipment, the use of dangerous chemical reagents in the reaction process, and pollution of

Peer review under responsibility of KeAi Communications Co., Ltd.
* Corresponding author. State Key Laboratory for Conservation and Utilization of Subtropical Agro-bioresources, Guangxi Research Center for Microbial and Enzyme Engineering Technology, College of Life Science and Technology, Guangxi University, Nanning, 530004, China.
E-mail address: jiangcj0520@gxust.edu.cn (C. Jiang).

https://doi.org/10.1016/j.synbio.2024.01.002
Received 29 September 2023; Received in revised form 27 December 2023; Accepted 4 January 2024
Available online 6 January 2024

the environment [7]. The production of dopamine is not sufficient to meet medical or industrial needs. Therefore, finding a more economical and efficient way to produce dopamine has become a current scientific research hotspot.

In the synthesis of natural dopamine, microbial fermentation has good attributes such as short fermentation cycle and reduced environmental pollution. The common intestinal bacteria such as *Escherichia coli* [8,10] and *Enterococcus faecium* [9] could also produce dopamine. Shishov et al. found that the culture fluid of *E. coli* contained nanomolar of dopamine during the late growth phase [8]. In addition, the yield of dopamine for *E. faecium* ML1082 was 133 μg/mL [9]. However, the synthesis of dopamine by these intestinal microorganisms e.g. *Enterococcus faecium* are in small amounts and mostly requires exogenous addition of the metabolic precursor dopa for dopamine synthesis [9], which poses an obstacle to efficient biosynthesis of dopamine in one step fermentation. Therefore, identifying high efficiently microorganisms in biosynthesize dopamine using low-cost raw materials in large-scale seems urgent [10]. However, few reports of natural biosynthesis of dopamine by the fungal yeast are found. The yeast *Meyerozyma guilliermondii*, which has natural physiological metabolic advantages, as a model organism for studying the dopamine metabolic process can help us better understand the metabolic regulation and catalytic mechanisms involved in dopamine synthesis in fungal yeast. At present, the metabolic regulation and catalytic mechanism of dopamine synthesis in *Meyerozyma guilliermondii*, especially under environmental stress conditions, are still kept unclear.

In addition to clinical medical applications, dopamine is involved in a variety of other important roles, such as the stress responses. Dopamine participates in the process of plant growth and development, and helps plants withstand multiple abiotic stresses by regulating the expression of stress-related genes. Furthermore, both endogenous dopamine and exogenously applied dopamine have been shown to enhance tolerance to various stresses, such as salt stress [6,11,12]. Liang et al. reported that exogenous dopamine significantly increased the concentrations, uptake, and transport of nutrients under drought stress, and also altered their distribution within the whole plant [13]. Ahmad et al. reported that dopamine alleviated hydrocarbon stress in *Brassica oleracea* through modulation of physio-biochemical attributes and antioxidant defense systems [14]. Jiao et al. reported that the presence of dopamine significantly alleviated the effects of alkali stress and the application of exogenous dopamine increased the antioxidant capacity of apple seedlings under alkali stress by increasing the level of chlorogenic acid [11]. Gao et al. reported that dopamine regulated the expression of genes related to metabolism of nitrogen, secondary compounds, and amino acids under drought stress [6]. However, the expression levels of dopamine in microorganisms under extreme environments and the differences in the expression of genes and proteins associated with its synthesis have been rarely reported.

In our previous studies, a novel marine multi-stress-tolerant aromatic yeast *Meyerozyma guilliermondii* GXDK6 with abundant amino acid metabolism genes was identified from subtropical marine mangrove microorganisms, which showed excellent salt-tolerant survivability [15]. Based on its typical physicochemical characteristics, GXDK6 had unique regulatory network of amino acid metabolism under NaCl stress, which could produce a variety of natural functional amino acid metabolites. To date, few reports had been found on the natural fermentation of dopamine synthesis by yeast. We hypothesized that *M. guilliermondii* GXDK6 had the potential for biosynthesis of dopamine using low-cost raw materials (such as glucose or sucrose) as the substrate. The expression level of dopamine was significantly increased when GXDK6 was exposed to high salt stress to alleviate the damage caused by salt stimulation. For the test of this hypothesis, the fermentation products were analyzed by gas chromatography-mass spectrometry (GC-MS) and high-performance liquid chromatography (HPLC), and the key proteins regulating dopamine synthesis in the whole genome of GXDK6 were deeply explored to reveal the key amino acid residues and map the pathway of dopamine metabolism in yeast. In addition, a combination of transcriptomic and proteomic data was used to systematically reveal the differences in dopamine metabolism of *M. guilliermondii* GXDK6 under salt stress. This study provided new insights into the metabolic differences regulating dopamine synthesis under high salt stress.

2. Materials and methods

2.1. Experimental strain

The fungal yeast *M. guilliermondii* GXDK6, which was obtained from the subtropical marine mangrove microorganisms, was released in the China General Microbiological Culture Collection Center (CGMCC) with the preservation number CGMCC No.16007.

2.2. Multi-omics analysis of M. guilliermondii GXDK6

Genome-wide profiling in *M. guilliermondii* GXDK6. CTAB method was used to extract the whole genomic DNA of *M. guilliermondii* GXDK6, and the purity of the extracted DNA was verified by PCR (Polymerase Chain Reaction) and agarose gel electrophoresis. The whole-genome sequencing data of GXDK6 were deposited in the National Microbiology Data Center database (see footnote 1) under accession number NMDC60014229 [15].

Transcriptome profiling in *M. guilliermondii* GXDK6. The trizol method was used to extract the total RNA of GXDK6 cultured at different salt concentrations (0 %, 5 %, and 10 % NaCl) (Trizol reagent kit, Invitrogen, Carlsbad, CA, USA) [16]. Sequencing was performed using Illumina HiSeq2500 by Gene Denovo Biotechnology Co. (Guangzhou, China). DESeq2 was used to analyze the differential expression of RNAs [17,18]. The genes/transcripts with the parameter of false discovery rate (FDR) below 0.05 and absolute fold change (FC) ≥ 2 were considered differentially expressed genes/transcripts. The RNA-Sequencing data of GXDK6 under NaCl stress had been deposited in GenBank with the accession number PRJNA752222.

Proteomic profiling in *M. guilliermondii* GXDK6. Samples from the same batch used for transcriptome sequencing were analyzed simultaneously for proteomic data. SDT Lysis method was used to extract the proteins in GXDK6 at different salt concentrations (0 %, 5 %, and 10 % NaCl) from three biological replicates of each sample and separated on 12.5 % SDS-PAGE gel [19]. Sequencing of the extracted proteins was conducted using a tandem mass tag (TMT)-based quantitative proteomics [20]. Proteins with FC > 1.2 and p-value (Student's t-test) < 0.05 were considered to be differentially expressed proteins (Detailed methods were described in Sun et al. [21]).

To assess the potential relevance of quantitative information between mRNA and proteins, the cut off values (DEGs: $|$Fold change (FC)$| > 2.0$ and FDR ≤ 0.001; DEPs: p-value < 0.05 and $|FC| > 1.20$) were used to screen the subsets of mRNA and proteins with apparent expression. Then, we used RNA-seq data as a searchable database, all identified protein sequences were analyzed and queried with the RNA-seq data. To further dig out the information from proteomes, the correlation analysis was conducted between DEPs and the whole transcript database.

2.3. Detection of dopamine by gas chromatography-mass spectrometry (GC-MS)

GXDK6 was cultured in YPD medium for 48 h and then centrifuged at 12, 000 rpm for 10 min to remove the cell sediment. The supernatant was filtered using a 0.22 μm sterile filter membrane, concentrated through refrigerated centrifugation (Shanghai, China), and then freeze-dried into powder. First, alkylation reaction of the samples was performed by adding 80 μL methoxyamine pyridine hydrochloride solution (a special reagent for GC analysis) with a concentration of 20 mg/mL and then oscillating in a rotary shaker at 200 rpm and 37 °C for 120 min.

Second, when the alkylation reaction was completed, 80 μL of MSTFA was added in the samples for derivatization reaction, which was also conducted in a rotary shaker at 200 rpm and 37 °C for 120 min. Subsequently, the samples were centrifuged at 12, 000 rpm for 10 min to collect the supernatant for GC–MS detection. The metabolites were detected and analyzed using GC–MS according to Pautova et al. [22] and Cai et al. [23], with slightly modifications.

2.4. Detection of dopamine content in *M. guilliermondii* GXDK6 based on HPLC

Dopamine standards were diluted using anhydrous ethanol (chromatographic grade) and standard curves were plotted (range 1–100 mg/L). The dopamine content was measured using HPLC when GXDK6 was incubated for 16 h at 0 %, 5 %, and 10 % NaCl, respectively (culture conditions: protected from light). 9 mL of samples was aspirated, quenched under liquid nitrogen, and then dried to powder using a centrifugal concentrator (SCIENTZ-1LS, China). After drying, 1 mL of the anhydrous ethanol was added to each tube of the sample, which was then mixed well and macerated by shaking (30 °C, 200 rpm). The supernatant after maceration was obtained by centrifugation at 12, 000 rpm for 10 min and subsequently filtered using a 0.22 μm filter membrane. The HPLC (WATERS, E2695, USA) was equipped with a Commasil TM C18 column (4.6 mm × 250 mm, 5 μm) and a 2998 PAD detector. Detection conditions: mobile phase 100 % methanol: 1 ‰ phosphoric acid solution = 20:80, flow rate 0.8 mL/min, column temperature 30 °C, loading volume 10 μL, detection wavelength 220 nm. Each group of samples was set up in 3 parallel.

2.5. Effect of adding exogenous dopamine on the growth of *M. guilliermondii* GXDK6

M. guilliermondii GXDK6 was cultured in YPD liquid medium containing 0 %, 5 %, and 10 % NaCl with 1 mg/L exogenous dopamine and without exogenous dopamine as a control. Subsequently, the OD_{600} was detected to evaluate the effect of adding exogenous dopamine on the growth of *M. guilliermondii* GXDK6. In addition, GXDK6 was coated onto YPD solid medium with 1 mg/L exogenous dopamine under 0 %, 5 %, and 10 % NaCl, respectively, and without exogenous dopamine as a control (10^{-5} concentration of GXDK6). Then the colony morphology and number of GXDK6 were observed. Three biological replicates were set up for each group and were considered significantly different at $p < 0.05$ (*t*-test).

2.6. Sequence analysis of AST and CAO

To identify regions of structurally and/or functionally important, the amino acid residues of AST and CAO were analyzed using the ConSurf web server (http://consurf.tau.ac.il) [24]. The ConSurf server was a bioinformatics tool for estimating the evolutionary conservation of amino acid positions in a protein molecule based on the phylogenetic relations between homologous sequences. The BLAST in NCBI (https://blast.ncbi.nlm.nih.gov/Blast.cgi) was used to search for close homologous sequences. A multiple sequence alignment (MSA) of the homologous sequences was constructed using Clustal Omega (https://www.ebi.ac.uk/Tools/msa/clustalo/). The conservation scores were calculated using the Bayesian method (default). The continuous conservation scores were divided into a discrete scale of nine grades for visualization, from the most variable positions (grade 1) colored turquoise, through intermediately conserved positions (grade 5) colored white, to the most conserved positions (grade 9) colored maroon. The enzyme activity centre of the protein was predicted using PyMOL software.

2.7. Construction of the overexpression strain GXDK6:AAT2

The column-based yeast genomic DNA extraction kit (provided by SBS Genetech Co., Ltd., catalog number B518257) was used to extract the total DNA. The *AAT2* was amplified using a PCR reaction using the genome as a template (Supplementary Tables S1, S2, and S3). The plasmid pPICZA was linearized by reverse amplification PCR using primers (Supplementary Tables S1, S2, and S3). The PCR product was purified and recovered using a PCR purification kit (Vazyme Biotech Co., Ltd., catalog number DC301). The purified product was subjected to 1 % agarose gel electrophoresis for identification. The linearized plasmid obtained above was ligated with the target gene using seamless cloning to obtain the recombinant plasmid pPICZA-AAT2 (Supplementary Table S4). The constructed recombinant plasmid was transformed into *E. coli* DH5α cells for amplification, and the positive transformants were obtained by colony PCR. The positive transformants were cultured in LB medium containing 25 μg/mL zeocin for 12 h, and the recombinant plasmids were extracted. The accuracy of the recombinant plasmids was verified by amplifying pPICZA and *AAT2* in PCR reactions using the extracted recombinant plasmids as templates. Subsequently, the recombinant plasmids were transformed into *M. guilliermondii* GXDK6 receptive cells by the lithium acetate method. Positive transformants were selected by PCR of fungal colonies and cultured in YPD liquid medium containing 1000 μg/mL zeocin. The dopamine content of GXDK6 and GXDK6AAT2 was detected by HPLC, respectively. The protein concentration and AST enzyme activity were detected using a BCA assay kit (Beyotime Biotechnology Co., Ltd., catalog number PC0020) and an AST kit (Nanjing Jiancheng Bioengineering Institute, catalog number C010-2-1). Each group of samples was set up in 3 parallel.

2.8. RT-qPCR analysis

To assess the RNA-seq quality, the same set of RNAs for RNA-seq were subjected to a two-step RT-qPCR assay with high-throughput real-time fluorescence quantitative PCR instrument (ROCHE 480II, Switzerland) using SYBR green RT-PCR kit (Yifeixue Biotechnology Co., Ltd., YFXM0001/2/3). The genes (*AO-I*, *AAT2*, and *ARO4*) which regulated dopamine metabolism and the other five genes (*CAR1*, *ARO10*, *URE2*, *RNR2*, and *HPD*) involved in the metabolism of amino acids above eight genes from the DEGs were selected for RT-qPCR to verify the accuracy and reproducibility of the RNA-Seq data (The forward and reverse primers were provided in Supplementary Table S5). The internal reference gene was *ACT*. Three sets of parallel trials were set up for each gene. The relative FC in target gene expression was calculated using the $2^{-\Delta\Delta Ct}$ method [25]. In addition, expression levels of genes in the dopamine metabolic pathway in GXDK6 and GXDK6AAT2 were also analyzed based on RT-qPCR as described above (The forward and reverse primers were provided in Supplementary Table S6).

2.9. Statistical analysis of data

The experimental data were processed with SPSS 25, Excel 2019, TBtools, the PyMOL Molecular Graphics System (1.7.2.1), and Diamond software. The relevant query databases were UniProt, SWISS-MODEL, KEGG, and NCBI. Significant difference was set at $p < 0.05$.

3. Results

3.1. Dopamine was synthesized by *M. guilliermondii* GXDK6

In order to explore the metabolites in *M. guilliermondii* GXDK6, a non-targeted metabolomics study was performed using a Gas chromatograph-mass spectrometer (GC-MS). For increasing the volatility of the sample or improving the detection sensitivity, the sample was derivatized before instrument injection. The results showed that dopamine was quantified with the peak time of 16.245 min and the peak area of 5, 914, 857, indicating that marine mangrove-derived

M. guilliermondii GXDK6 could be used to obtain dopamine from glucose fermentation without engineering. The hydrogen on the hydroxyl group and amino group were replaced by trimethylsilane (TMS) after the derivatization of dopamine. At this time, the chromatographic behavior was good. The mass spectrum of the derived dopamine was shown in Fig. 1. The mass spectra showed that the derivatives of dopamine had characteristic ions at *m/z* 116.9, 146.9, 173.9, 206.8, and 298.8, and the proportional relationships of these fragment ions could be used for the qualitative analysis of dopamine. The quantified ion was used at *m/z* 173.9, because this characteristic ion had a certain abundance and was less disturbed by impurities. This was the first report on the synthesis of dopamine by fermentation in fungal yeast.

3.2. The proposed pathway of dopamine in M. guilliermondii GXDK6 revealed by the whole genome wide analysis

40 % sequence identity were used as a confident threshold for assessing functional conservation because functional variation was rare when the sequence identity was above 40 % [26]. Catechol-*O*-methyltransferase (COMT) was the major enzyme determining cortical dopamine flux [27]. Based on the genome-wide data, by comparing the COMT sequence in *M. guilliermondii* GXDK6 with that in *Candida albicans* P94015 (sequence ID: KGQ82201.1), 51.3 % sequence identity was observed, speculating that *M. guilliermondii* GXDK6 had the potential to express COMT (encoded by *COMT*, scaffold8.t127) and thus further metabolize dopamine. In addition, copper amine oxidase encoded by *AO-I*, which was involved in the metabolism of dopamine [28], was expressed in *M. guilliermondii* GXDK6. Therefore, it was speculated that *M. guilliermondii* GXDK6 had the potential to biosynthesize dopamine.

Fourteen genes (*ARO4*, *ARO1*, *ARO2*, *ARO7*, *TYR1*, *AAT2*, *ARO8*, *HIS5*, *CYP76AD1*, *mfnA*, *AO-I*, *COMT*, *FMS1,* and *ALDH*) through sequence alignment with functional proteins had been demonstrated relating with dopamine metabolism. Then the proposed pathway of dopamine in *M. guilliermondii* GXDK6 had been constructed successfully (as shown in Fig. 2A) [29]. D-Erythrose 4-phosphate had been found to be converted into 3-deoxy-D-arabino-heptulosoate 7-phosphate (DAHP) under the action of 3-deoxy-7-phosphoheptulonate synthase (encoded by *ARO4*). AROM protein (encoded by *ARO1*), which catalyzed 5-step consecutive enzymatic reactions to convert DAHP to 5-*O*-3-phosphoshikimate. 5-*O*-3-phosphoshikimate synthesized chorismate under the action of chorismate synthase (encoded by *ARO2*), and then chorismate was converted into prephenate under the action of chorismate mutase (encoded by *ARO7*). Then prephenate was then converted to 4-hydroxyphenylpyruvate by the action of prephenate dehydrogenase (encoded by *TYR1*), followed by further production of L-tyrosine under the combined action of aspartate aminotransferase (AST, encoded by *AAT2*), aromatic amino acid aminotransferase I (encoded by *ARO8*), and histidinol-phosphate transaminase (encoded by *HIS5*), respectively. Tyrosine was further converted to L-dopa (*CYP76AD1* was the regulatory gene) [30]. Tyrosine decarboxylase (encoded by *mfnA*) was one of the key enzymes in the catecholamine biosynthesis pathway, which could catalyze the synthesis of the neurotransmitter dopamine from L-dopa. Meanwhile, dopamine was converted to 3,4-dihydroxyphenylacetaldehyde by the action of copper amine oxidase (CAO, encoded by *AO-I*). Further, the dopamine synthesized in *M. guilliermondii* GXDK6 was catalyzed by catechol O-methyltransferase (encoded by *COMT*) to 3-methoxytyramine. Subsequently, 3-methoxytyramine was transformed into 3-methoxy-4-hydroxyphenylacetaldehyde by monoamine oxidase (encoded by *FMS1*), and finally, 3-methoxy-4-hydroxyphenylacetaldehyde was catalyzed to homovanillic acid by aldehyde dehydrogenase (NAD(P)+) (encoded by *ALDH*).

Furthermore, network interaction analysis of the above genes revealed strong interactions among *ARO1*, *ARO2*, *ARO4, ARO7*, *ARO8*, *TYR1*, *HIS5*, and *AAT2*, while the interactions among other genes were not revealed in STRING (functional protein association networks), suggesting that new protein interaction networks were present in *M. guilliermondii* to participate in the metabolism of dopamine [31]. In addition, homovanillic acid is able to perform a variety of functions such as antioxidant, anti-inflammatory, and anti-tumor, which have a wide range of applications in medical, food and cosmetic fields [32]. It is hypothesized that dopamine or homovanillic acid natural synthesized by fermentation with low-priced glucose contributes to the stress tolerance of the yeast GXDK6 under environmental stress.

3.3. Multiple sequence alignment of aspartate aminotransferase and copper amine oxidase

In addition, according to the transcriptome data, the expression levels of *AAT2* and *AO-I* were significantly different under 10 % NaCl stress compared with no stress, so the AST for dopamine synthesis and CAO involved in dopamine catabolism were screened for multiple sequence alignment with homofunctional proteins, and conserved regions of the proteins, as well as key amino acid residues, were analyzed. AST generally forms a homodimer consisting of two active sites in the vicinity of subunit interfaces; these active sites bind to its cofactor PLP and substrate independently [33]. Researches showed that AST in *M. guilliermondii* GXDK6 had high homology with that of *Meyerozyma* sp. JA9 (RLV85771.1, 86.07 %), *Candida parapsilosis* (KAI5906130.1, 53.98 %), *Candida viswanathii* (RCK59576.1, 52.75 %), *Candida railenensis* (CAH2351020.1, 51.48 %), and *Metschnikowia aff. pulcherrima* (QBM85876.1, 50.38 %), respectively (Supplementary Fig. S1). The conserved sequences were Cys-His-Asn-Pro-Thr-Gly and Pro-Ala-Phe-Gly-Ala-Arg. The A chain of AST (PDB ID: 1YAA) was selected to show the conserved region of the protein with other sequences, and the results were shown in Fig. 2B, which visualized the position of the conserved region (red area) in the protein structure.

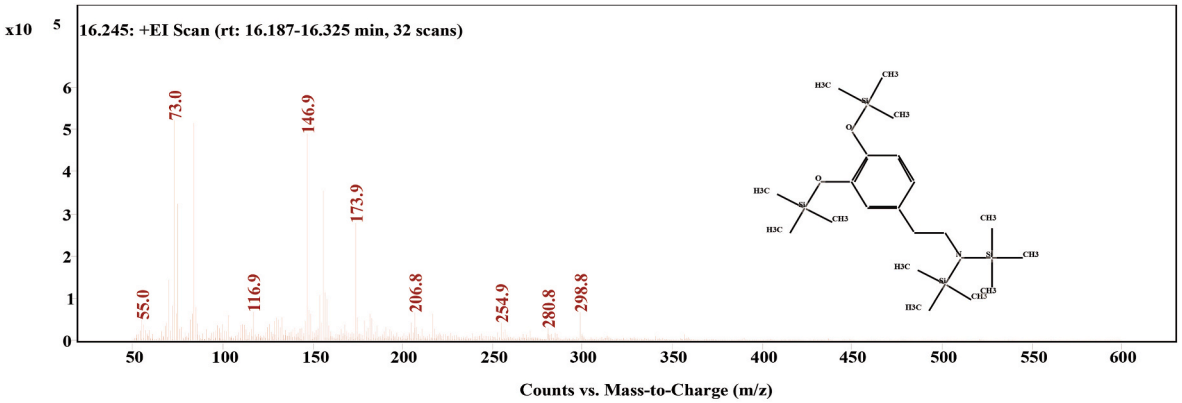

Fig. 1. Mass spectra of dopamine in *M. guilliermondii* (after derivatization).

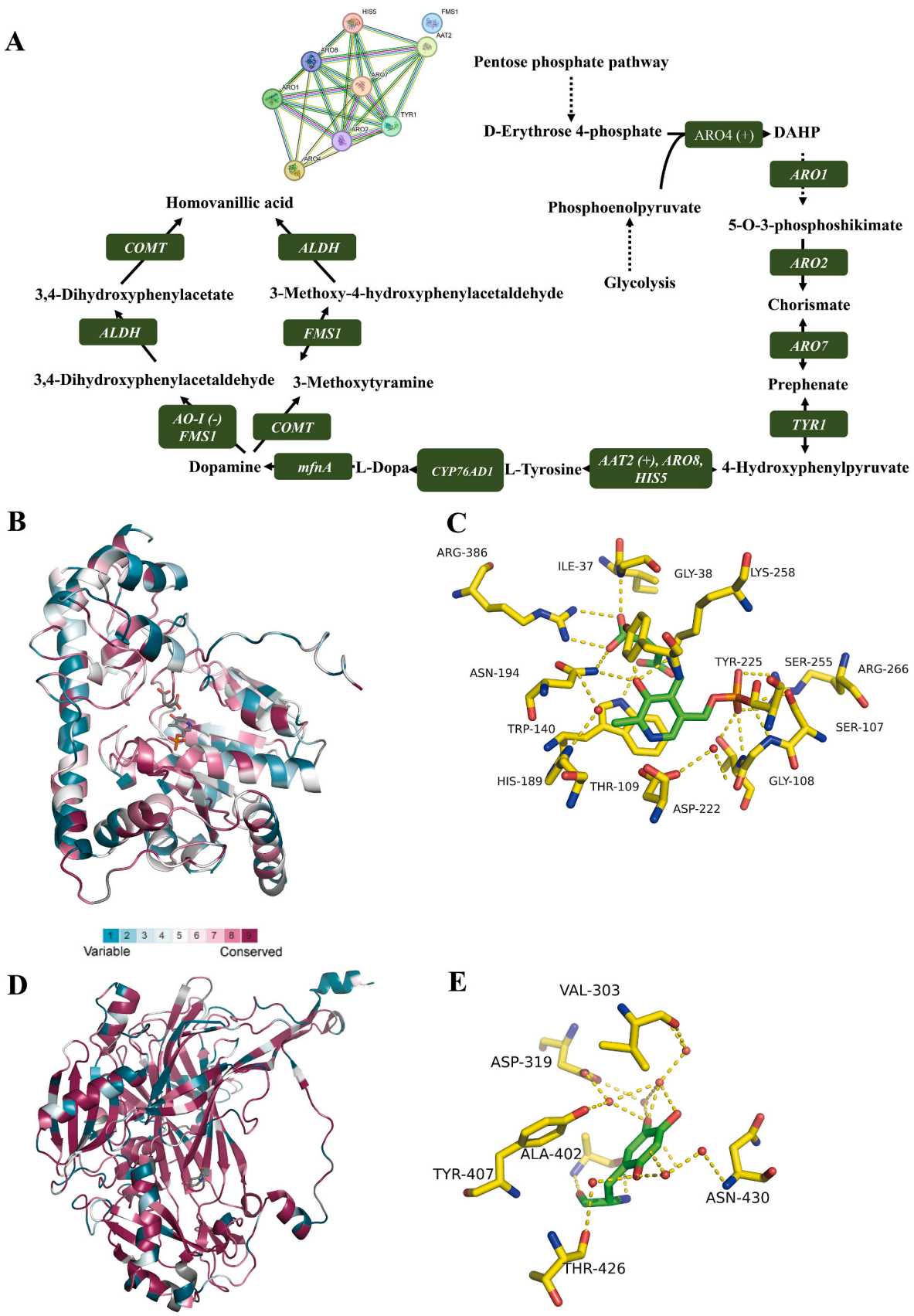

Fig. 2. The biosynthetic pathway of dopamine in *M. guilliermondii* GXDK6. (A) The biosynthetic pathway of dopamine; (B) The conserved sequences of aspartate aminotransferase; (C) The key amino acid residues of aspartate aminotransferase; (D) The conserved sequences of copper amine oxidase; (E) The key amino acid residues of copper amine oxidase.

Analysis of the active centre of the enzyme revealed that chemical small molecule ligands (within the 5A range) interacted with their targets through hydrogen bonding (polar interaction) and that water molecules 929 and 936 in the protein were involved in the formation of hydrogen bonds between the protein and the ligand. The key amino acid residues involved in hydrogen bonding were shown in Fig. 2C. The key amino acid residue sites of AST were identified as aspartic acid (Asp), asparagine (Asn), tyrosine (Tyr), and arginine (Arg). The analysis of the sites of key amino acid residues in the enzyme protein structure can lay the foundation for further investigation of the catalytic mechanism of AST protein in *M. guilliermondii* GXDK6.

In addition, multiple sequence alignment analysis revealed that CAO

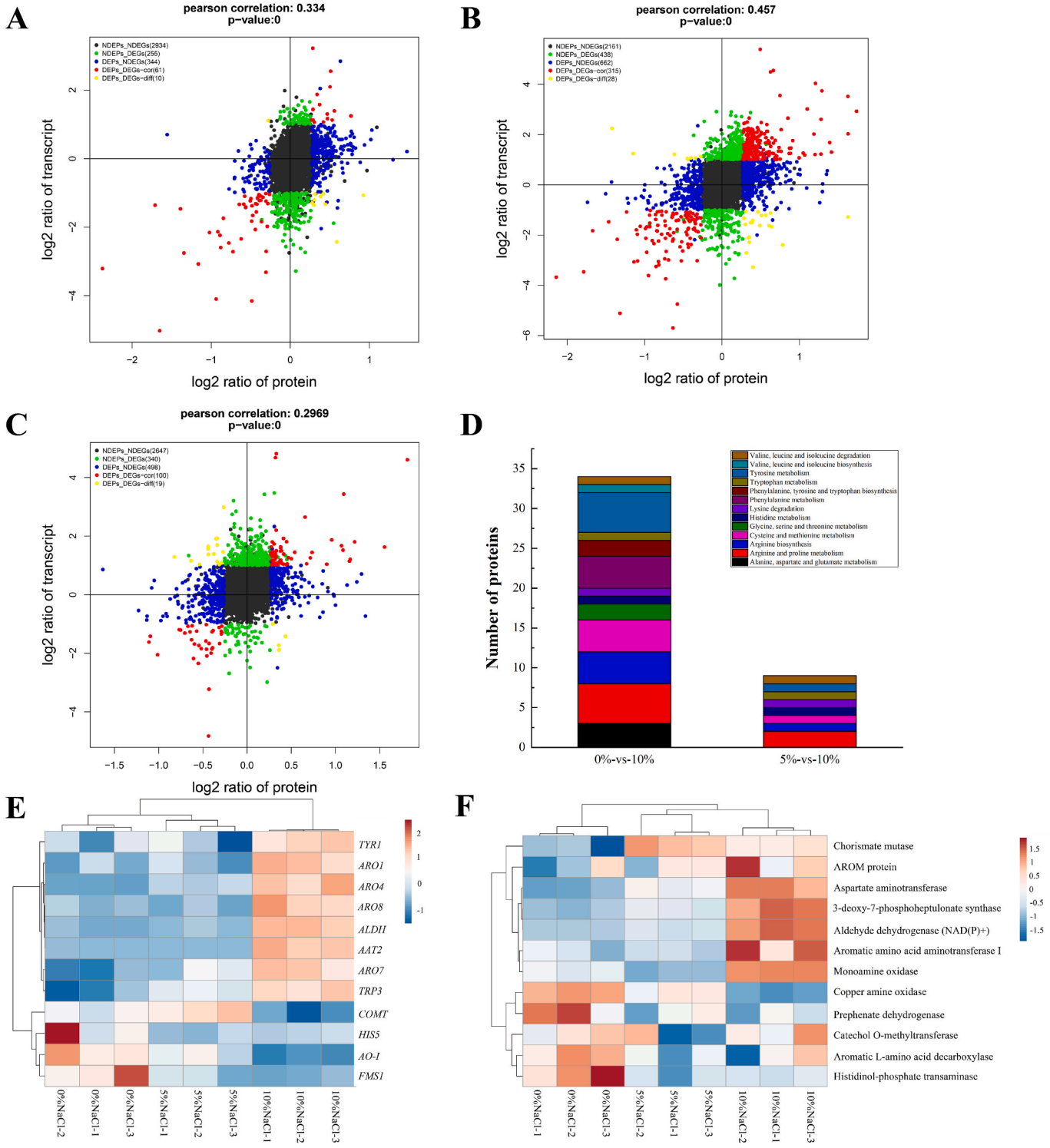

Fig. 3. Transcriptome and proteome reveal the expression levels of key genes regulating dopamine metabolism under NaCl stress. (A) Association analysis comparing transcriptome and proteome under 0 % and 5 % NaCl conditions; (B) Association analysis comparing transcriptome and proteome under 0 % and 10 % NaCl conditions; (C) Association analysis comparing transcriptome and proteome under 5 % and 10 % NaCl conditions; (D) Association analysis comparing transcriptome and proteome in amino acid metabolism; (E) Expression levels of key genes regulating dopamine metabolism revealed based on transcriptomic data; (F) Expression levels of key proteins regulating dopamine metabolism revealed based on proteomic data.

from *M. guilliermondii* GXDK6 had have high homology to *Schefferomyces stipitis* CBS 6054 (XP_001384892.1, 81.49 %), *Candida railenensis* (CAH2353551.1, 80.82 %), *Suhomyces tanzawaensis* NRRL Y-17324 (XP_020065782.1, 81.31 %), *Candida viswanathii* (RCK55058.1, 80.70 %), and *Candida albicans* P34048 (KGU28736.1, 78.39 %), indicating that the protein in *M. guilliermondii* GXDK6 had the same or similar functions to that of the other species compared above (regulation of dopamine metabolism), which had the same conserved sequence as Arg-Ala-Thr-Gly-Ile-Leu-Ser-Thr-Met-Pro-Ile-Asp-Glu-Asn-Val-Lys-Val-Pro-Trp-Gly-Thr-Ile-Val-Gly-Pro-Asn-Val-Met-Ala-Ala-Tyr-His-Gln-His-Ile-Leu (Supplementary Fig. S2). In addition, CAO encoded by *AO-I* were involved in the metabolism of xenobiotic and biogenic amines [34]. When Cu^{2+} as a cofactor, CAO can catalyze the oxidation of primary amines to aldehydes, while reducing dioxygen to hydrogen peroxide. The cofactor Cu^{2+} played a crucial role in the activity of CAO. The A chain of CAO (PDB ID: 3N9H) was selected to show the conserved region of the protein with other sequences, and the results were shown in Fig. 2D. Analysis of the active centre of the enzyme revealed that chemical small molecules (within the range of 5A) interacted with their targets through hydrogen bonding (polar interaction), and water molecules 1205, 1503, 1029, 1498, 1053, 1497, and 1499 in the protein were involved in the formation of hydrogen bonds between the protein and the small molecules.The key amino acid residue sites of CAO were aspartic acid and tyrosine. The key amino acid residues involved in hydrogen bonding were shown in Fig. 2E, which laid the foundation for the subsequent study of the catalytic mechanism of the CAO.

3.4. Integration of genome-wide, transcriptomic and proteomic data analysis revealed that NaCl stress contributed to the biosynthesis of dopamine in M. guilliermondii GXDK6

The transcriptome and proteome were used to investigate the differential regulation of dopamine metabolism in *M. guilliermondii* GXDK6 under NaCl stress. 5175 genes and 3604 proteins were identified in GXDK6, each protein was matched with their corresponding gene. The expression changes of genes in transcriptome and proteome were further divided and a four-quadrant diagram was constructed. Quantitative and enrichment analysis were performed on the genes in each quadrant of the four-quadrant diagram. In the four-quadrant diagram, the largest number of proteins (genes) were those with no differential expression at both transcript and translation levels, followed by those with differential expression at either the protein or mRNA level (Fig. 3). Compared to the 0 % NaCl condition, both non-differentially expressed proteins (NDEPs) and non-differentially expressed genes (NDEGs) were 2934, NDEGs with differentially expressed proteins (DEPs) were 344, differentially expressed genes (DEGs) with NDEPs were 255, DEGs with DEPs were 71 under 5 % NaCl condition (Fig. 3A). Compared to the 0 % NaCl condition, NDEPs with NDEGs were 2161, NDEGs with DEPs were 662, DEGs with NDEPs were 438, DEGs with DEPs were 343 under 10 % NaCl condition (Fig. 3B). Compared to the 5 % NaCl condition, NDEPs with NDEGs were 2647, NDEGs with DEPs were 498, DEGs with NDEPs were 340, DEGs with DEPs were 119 under 10 % NaCl condition (Fig. 3C). The above results indicated that the corresponding proteins (genes) at both transcriptional and translational levels were fewer revealed under NaCl stress, while more genes were expressed at a single level of transcription or translation, thereby promoting growth and metabolism of GXDK6 under NaCl stress, which was similar with Jia et al. [35].

Twelve DEGs and DEPs in amino acid metabolism were associated under 10 % NaCl (vs. 0 % NaCl) (Supplementary Table S7), while four DEGs and DEPs were associated under 10 % NaCl (vs. 5 % NaCl) (Supplementary Table S8). In addition, four DEGs and DEPs in the metabolism of other amino acids were associated under 10 % NaCl (vs. 0 % NaCl) (Supplementary Table S9), while one DEG and DEP was associated under 10 % NaCl (vs. 5 % NaCl) (Supplementary Table S10). The DEGs and DEPs associated with amino acid metabolism were involved in the regulation of tyrosine metabolism, arginine and proline metabolism, and phenylalanine metabolism (Fig. 3D). Annotated DEGs enriched in tyrosine metabolism (the primary pathway of dopamine metabolism) include *AO-I* (involved in dopamine degradation) and *AAT2* (involved in regulating dopamine synthesis). Therefore, it was speculated that salt stress affected the process of dopamine metabolism. The eight genes (*AO-I*, *AAT2*, *ARO4*, *CAR1*, *ARO10, URE2*, *RNR2*, and *HPD*) involved in the metabolism of amino acids from the DEGs were selected for RT-qPCR to verify the accuracy and reproducibility of the RNA-Seq data (Supplementary Fig. S3). The results showed that the expression trends of these genes were similar to those of RNA-seq, indicating the reliability of RNA-seq analysis.

Transcriptomic analysis revealed that *ARO4* (scaffold1.g160) was upregulated 1.02-fold under 5 % NaCl (vs. 0 % NaCl), 2.40-fold under 10 % NaCl (vs. 0 % NaCl), and 1.38-fold under 10 % NaCl (vs. 5 % NaCl), respectively (Fig. 3E). In addition, *AAT2* (scaffold3.g530) was downregulated 0.27-fold under 5 % NaCl (vs. 0 % NaCl), while *AAT2* was upregulated 4.54-fold under 10 % NaCl (vs. 0 % NaCl), and 4.81-fold under 10 % NaCl (vs. 5 % NaCl), respectively. *ARO4* and *AAT2* contributing to dopamine biosynthesis were significantly upregulated in *M. guilliermondii* GXDK6 under 10 % NaCl. Meanwhile, *AO-I* (scaffold1.g90), which promotes dopamine catabolism, was downregulated 0.70-fold under 5 % NaCl (vs. 0%NaCl), 3.06-fold under 10 % NaCl (vs. 0% NaCl), and 2.35-fold under 10 % NaCl (vs. 5%NaCl), respectively. Proteomic analysis showed that aspartate aminotransferase (AST, encoded by *AAT2*) was upregulated 0.33-fold under 5 % NaCl (vs. 0 % NaCl), 0.66-fold under 10 % NaCl (vs. 0 % NaCl), and 0.33-fold under 10 % NaCl (vs. 5 % NaCl), respectively. Meanwhile, copper amine oxidase (encoded by *AO-I*) was downregulated 0.27-fold under 5 % NaCl (vs. 0 % NaCl), 0.83-fold under 10 % NaCl (vs. 0 % NaCl), and 0.56-fold under 10 % NaCl (vs. 5 % NaCl), respectively ($p < 0.05$) (Fig. 3F). Dopamine was characterized as a strong water-soluble antioxidant with higher anti-oxidative capability than glutathione, contributing to the normal growth of microorganisms under NaCl stress. Transcriptomic data showed that genes (e.g. *AAT2* and *AO-I*) regulating dopamine metabolism were significantly differentially expressed under salt stress, and proteomic data obtained from the same fermentation batch showed a corresponding trend of differential expression. The integrated multi-omics analysis showed that the genes or proteins involved in dopamine synthesis and catabolism had the same change pattern, which revealed the regulatory influence mechanism between gene expression and protein, contributing to the mechanism of dopamine biosynthesis in *M. guilliermondii* GXDK6 under salt stress.

3.5. The amount of dopamine biosynthesized by M. guilliermondii GXDK6 was increased after perceived salt stress

Dopamine content was assayed using HPLC when GXDK6 was incubated at 0 %, 5 %, and 10 % NaCl for 16 h, respectively (Fig. 4A and B). The results showed that the concentration of dopamine reached 29.00 mg/L when *M. guilliermondii* GXDK6 was not stressed, 62.01 mg/L under 5 % NaCl stress, and 72.83 mg/L under 10 % NaCl stress, respectively. The amount of dopamine synthesized by *M. guilliermondii* GXDK6 under 10 % NaCl stress was 2.51-fold higher than that of no stress. Multi-omics analysis revealed that the synthesis of dopamine increased under salt stress. The results of HPLC also confirmed the conclusions from the multi-omics analysis. The final results demonstrated that NaCl stress contributed to the synthesis of dopamine, considering that dopamine, a strong water-soluble antioxidant, was beneficial to alleviating oxidative stress caused by excessive oxygenation due to NaCl stress [36].

Furthermore, it was found that exogenous addition of dopamine contributed to enhancing the growth of GXDK6 under high NaCl stress, and the results were shown in Fig. 4C ($p < 0.05$). Under 0 % NaCl and 1 mg/L exogenous dopamine, the OD_{600} of GXDK6 was 1.57 after 16 h, which was 5.37 % higher than that under 0 % NaCl and no dopamine. Under 5 % NaCl and 1 mg/L exogenous dopamine, the OD_{600} of GXDK6

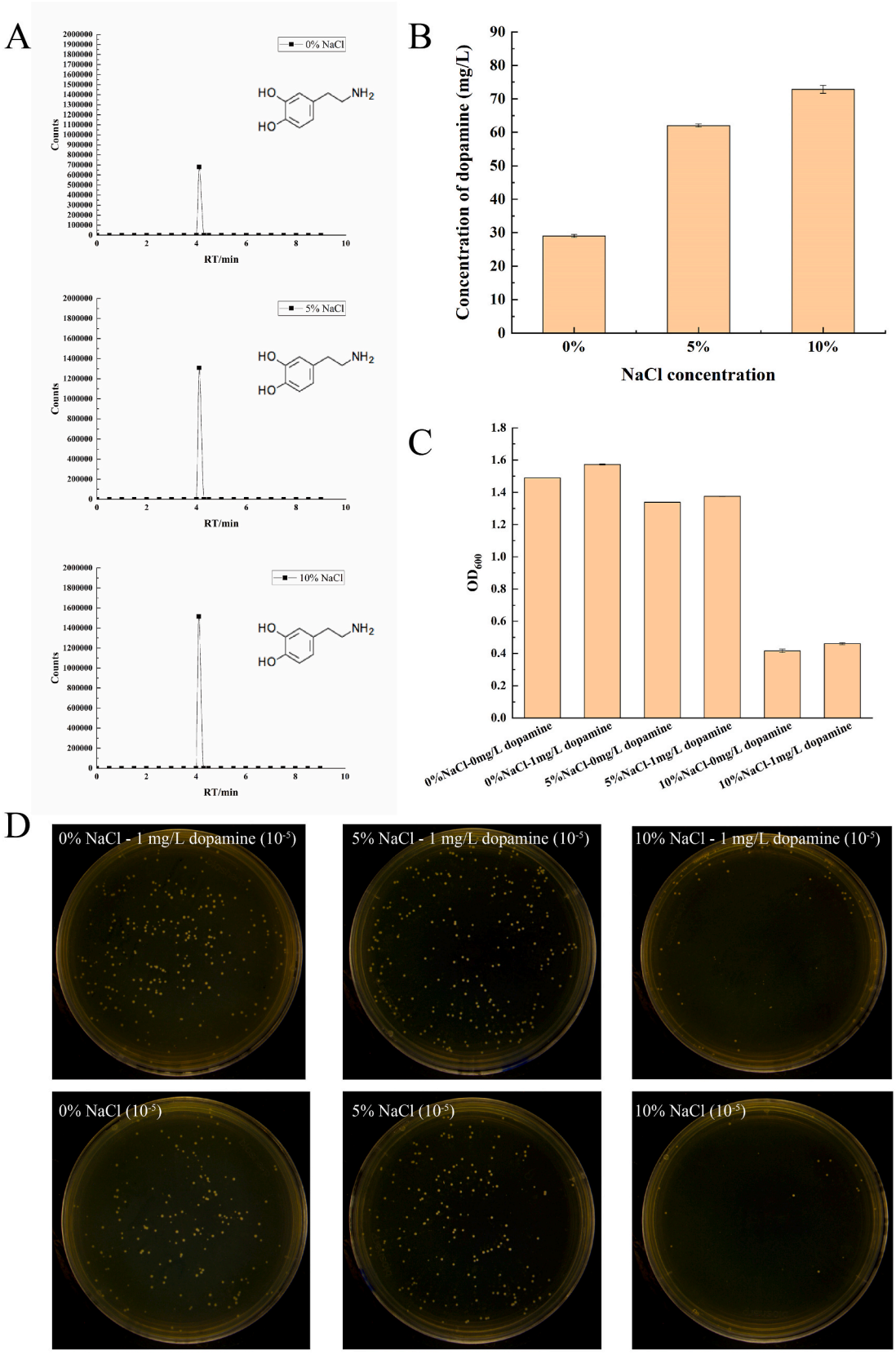

Fig. 4. The amount of dopamine biosynthesized by *M. guilliermondii* GXDK6 at 0 %, 5 %, and 10 % NaCl respectively by HPLC. (A) Chromatograms of dopamine biosynthesized by *M. guilliermondii* GXDK6 at 0 %, 5 %, and 10 % NaCl, respectively; (B) The amount of dopamine biosynthesized by *M. guilliermondii* GXDK6 after 16 h of fermentation with 0 %, 5 %, and 10 % NaCl, respectively; (C) Effect of exogenous addition of dopamine on the growth of *M. guilliermondii* GXDK6 at 0 %, 5 %, and 10 % NaCl, respectively; (D) Effect of exogenous addition of dopamine on the colony morphology for *M. guilliermondii* GXDK6 at 0 %, 5 %, and 10 % NaCl, respectively.

was 1.38 after 16 h, which was 2.99 % higher than that under 5 % NaCl and no dopamine. Meanwhile, under 10 % NaCl and 1 mg/L exogenous dopamine, the OD_{600} of GXDK6 was 0.46 after 16 h, which was 9.52 % higher than that under 10 % NaCl and no dopamine. In addition, the number of colonies under 5 % and 10 % NaCl was 93.19 % and 7.96 % of that under 0 % NaCl, respectively, indicating a significant inhibition of growth under 10 % NaCl. Further analysis revealed the number of colonies were increased by 17.24 %, 16.70 %, and 108.89 % under 0 %, 5 %, and 10 % NaCl, respectively, when 1 mg/L dopamine was added (Fig. 4D and Supplementary Table S12). These findings highlighted the potential of exogenously added dopamine in promoting growth under different salt stresses, with the highest enhancement observed under 10 % NaCl. A significant role of dopamine was further demonstrated in mitigating the impact of high salt stress upon the growth of GXDK6 by reducing oxidative stress. Liu et al. reported that endogenous or exogenous application of dopamine improved the tolerance against several abiotic stresses, such as drought, salt, and nutrient stress, which was similar to our results [37].

3.6. GXDK6:AAT2 strain enhanced AST enzyme activity and thus further stimulated the dopamine production

AAT2 was inserted into pPICZA vector to construct the recombinant plasmid, which was subsequently introduced into GXDK6 to construct GXDK6AAT2 (as shown in Fig. 5A). The linearized vector pPICZA (3323 bp) and *AAT2* gene fragment (1209 bp) were obtained through PCR amplification (Supplementary Fig. S4). These two fragments were seamlessly ligated using cloning techniques to generate the recombinant plasmid. The recombinant plasmid was amplified after being transferred into the *E. coli* DH5α. Subsequently, *AAT2* was amplified by colony PCR to screen for positive transformants (the positive transformants contained pPICZA-AAT2), and the results were shown in Fig. 5C, which showed a bright band of 1209 bp size. The recombinant plasmid extracted from the positive transformants was used as a template to amplify the pPICZA and *AAT2* to verify the accuracy of the recombinant plasmid again, and the results were shown in Supplementary Fig. S5, which showed bright band of 3323 bp and 1209 bp, respectively, indicating that the recombinant plasmid pPICZA-AAT2 had been successfully obtained. The recombinant plasmid was further introduced into GXDK6 to overexpress gene *AAT2* (Fig. 5D). Furthermore, compared with GXDK6, the total protein concentration in GXDK6AAT2 was increased by 6.28 % (Fig. 5B), additionally, the enzyme activity of AST in GXDK6AAT2 was increased by 24.89 % (Fig. 5F). Moreover, the dopamine production in GXDK6AAT2 was stimulated and increased by 56.36 % (Fig. 5E). The RT-qPCR results showed that the overexpression of *AAT2* led to an increase in the expression level of other related genes, which enhanced the expression of other genes in the dopamine metabolic pathway, resulting in a more vigorous dopamine metabolism and further accumulation of dopamine (Fig. 5A). The overexpression of *AAT2* also further verified the regulatory mechanism of dopamine metabolism.

4. Discussion

Dopamine is a precursor substance for the biosynthesis of many natural antioxidant drugs, acting as a neurotransmitter in the human body to regulate various physiological functions of the central nervous system, which is commonly used in the clinical treatment of many types of shock. At present, de novo synthesis of dopamine has been achieved through microbial synthesis technology, but the synthesis efficiency is very low [38]. In this study, the wild yeast *M. guilliermondii* GXDK6 was separated from marine mangrove microorganisms, which could biosynthesize dopamine using a low-valent carbon source (glucose) as a metabolic precursor substance. The process of dopamine was efficient and simple, contributing to the large-scale production.

The expression profiles of genes regulating dopamine metabolism in *M. guilliermondii* GXDK6 under NaCl stress were systematically revealed by multi-omics techniques (whole genome, transcriptome, and proteome). Through whole-genome analysis, *CYP76AD1* mediates tyrosine hydroxylation to form dopa, and further catalyzes to dopamine. Dopamine synthesized by GXDK6 using glucose can be catalyzed by catechol O-methyltransferase, monoamine oxidase, and aldehyde dehydrogenase (NAD(P)+) to synthesize homovanillic acid. Transcriptome and proteome analysis found that *AAT2* and its encoded enzyme AST promoting dopamine synthesis showed an upward trend of expression under NaCl stress, while *AO-I* and its corresponding enzyme CAO which regulated dopamine degradation showed a downward trend, which reduced the degradation of dopamine thereby accumulating. Self-synthesized dopamine (a strong water-soluble antioxidant) was used to attenuate the oxidative stress produced by NaCl stress. HPLC results showed that the production of dopamine increased under salt stress, verifying the accuracy of the multi-omics results. At present, the biosynthesis of dopamine by *E. coli* had been reported, but the synthesis of dopamine by yeast has not yet been found. This study has revealed for the first time that *M. guilliermondii* GXDK6 has the ability to biosynthesize dopamine, while the genes and proteins regulating dopamine synthesis have been mined, expanding the gene pool of dopamine metabolism, and providing a new source for dopamine acquisition. Moreover, the association between NaCl stress and dopamine metabolism was comprehensively revealed by integrated multi-omics techniques. This study also provides a new idea to construct a chassis cell factory for dopamine biosynthesis based on *M. guilliermondii* GXDK6.

The total synthesis content was detected using HPLC after 16 h incubation at different salt concentrations. The results showed that the concentration of dopamine reached 29.00 mg/L when *M. guilliermondii* GXDK6 was not stressed, 62.01 mg/L under 5 % NaCl stress, and 72.83 mg/L under 10 % NaCl stress, respectively. Moreover, the extracellular dopamine content was detected using HPLC on the fermentation broth (measuring the extracellular secretion content) after 16 h incubation at different salt concentrations. The results showed that the extracellular concentration of dopamine reached 18.66 mg/L when *M. guilliermondii* GXDK6 was not stressed, 13.65 mg/L under 5 % NaCl stress, and 12.50 mg/L under 10 % NaCl stress (dopamine peak time in the range of 3.266 ± 0.05, respectively) (Supplementary Table S11). Therefore, the intracellular concentration of dopamine reached 10.34 mg/L when *M. guilliermondii* GXDK6 was not stressed, 48.36 mg/L under 5 % NaCl stress, and 60.33 mg/L under 10 % NaCl stress, respectively. With the NaCl stress increasing, the amount of dopamine accumulated in the cell increased and the amount excreted outside the cell decreased. It is natural suggested that NaCl stress causes an increase in intracellular reactive oxygen species (ROS), which triggers an intracellular oxidative stress response [39]. Dopamine, a strong water-soluble antioxidant under NaCl stress, could accumulate in large amounts intracellularly and reduces efflux, thereby alleviating the oxidative stress response induced by high salt stimulation, enhancing the redox capacity of cells, contributing to maintain intracellular redox homeostasis, and protecting cells from oxidative damage [40]. The final results showed that the addition of dopamine or the increase of endogenous dopamine synthesis contributed to the growth and metabolism of *M. guilliermondii* GXDK6 under salt stress.

5. Conclusions

Genes regulating dopamine metabolism were identified and the differential expression profiles of these genes under NaCl stress were investigated with the genome-wide, transcriptomic, and proteomic analyses. GC-MS qualitatively revealed that GXDK6 had the ability to biosynthesize dopamine using glucose in natural fermentation. Based on the whole genome sequence analysis, 14 genes on dopamine metabolism were annotated. Multi-omics analysis revealed that NaCl stress contributed to dopamine accumulation, which was further confirmed by high performance liquid chromatography. Self-biosynthesized

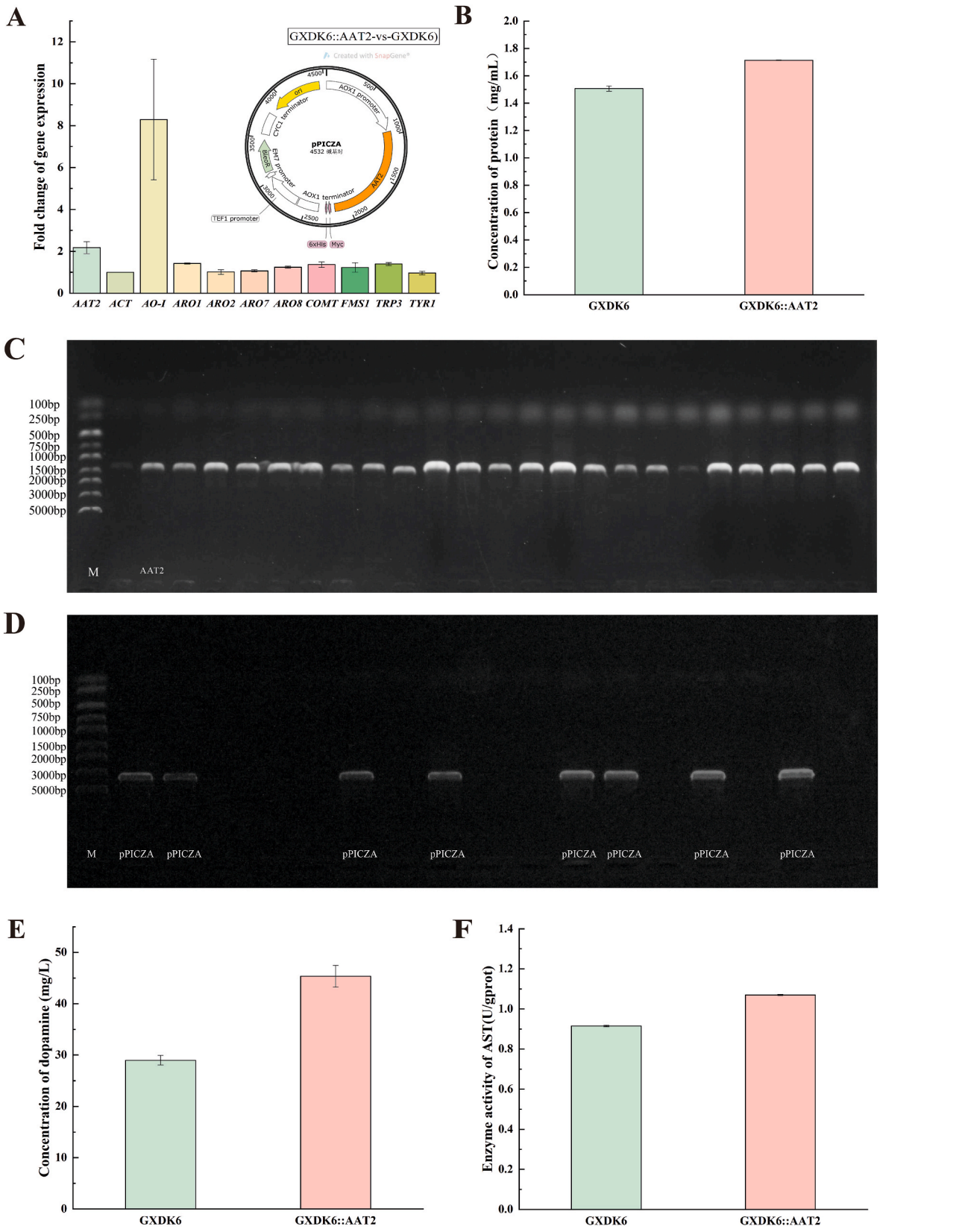

Fig. 5. Overexpression of *AAT2* in *M. guilliermondii* GXDK6. (A) Expression levels of other related genes in dopamine metabolism pathway in GXDK6AAT2 as compared to GXDK6; (B) Protein concentration in GXDK6 and GXDK6AAT2; (C) PCR electropherogram of colonies for positive transformants of *E. coli*; (D) PCR electrophoresis of colonies for positive transformants of *M. guilliermondii* GXDK6; (E) Concentration of dopamine in GXDK6 and GXDK6 AAT2; (F) AST enzyme activity in GXDK6 and GXDK6AAT2.

dopamine was used as a strong water-soluble antioxidant to alleviate oxidative stress in *M. guilliermondii* GXDK6 after perceived NaCl stress. Exogenous addition of dopamine also showed that dopamine alleviated the damage caused by NaCl stress and promoted cell growth. Further, when the dopamine anabolism-regulated gene *AAT2* was overexpressed in GXDK6, the expression level of *AAT2* was increased and the enzyme activity of AST encoded by *AAT2* was enhanced, which led to the up-regulation of other genes of dopamine metabolism, resulting in an increase in dopamine synthesis. This study revealed the association between the regulatory mechanism of dopamine and NaCl stress in *M. guilliermondii*, and expanded the gene pool regulating dopamine synthesis, contributing to the efficient production of dopamine.

Funding

This research was supported by the Funding Project of Chinese Central Government Guiding to the Guangxi Local Science and Technology Development (Grant No. GUIKEZY21195021), the Natural Science Fund for Distinguished Young Scholars of Guangxi Zhuang Autonomous Region of China (Grant No. 2019GXNSFFA245011), the Funding Project of Chinese Central Government Guiding to the Nanning Local Science and Technology Development (Grant No. 20231012), the Funding Projects of Guangxi Key Research and Development Plan (GUIKE AB23075173), and the Funding Project of Technological Development from Angel Yeast (Chongzuo) Co., Ltd. (Grant No. JS1006020230722019).

Institutional review board statement

Not applicable.

Informed consent statement

Not applicable.

Data availability statement

This Whole Genome Shotgun project had been deposited at DDBJ/ENA/GenBank under the accession JAIGNZ000000000. The RNA-Seq of *M. guilliermondii* GXDK6 under NaCl stress had been deposited at GenBank under the accession PRJNA752222.

CRediT authorship contribution statement

Huijie Sun: conducted the experiments and wrote the manuscript. **Huashan Bai:** conducted the experiments and wrote the manuscript. **Yonghong Hu:** designed the study, corrected the language errors of the manuscript. **Sheng He:** designed the study, corrected the language errors of the manuscript. **Ruihang Wei:** conducted the experiments and revised the manuscript. **Duotao Meng:** arranged and analyzed the experimental data. **Qiong Jiang:** arranged and analyzed the experimental data. **Hongping Pan:** provided the technical support. **Peihong Shen:** provided the technical support. **Qian Ou:** provided the technical support. **Chengjian Jiang:** designed the study, conducted the experiments and revised the manuscript, provided theoretical direction of multi-omics research, corrected the language errors of the manuscript, All authors have read and agreed to the published version of the manuscript.

Declaration of competing interest

The authors declare that they have no known competing financial interests or personal relationships that could have appeared to influence the work reported in this paper.

Acknowledgments

The authors express their special gratitude to all the funding sources for the financial assistance and specially to Guangxi University.

Appendix A. Supplementary data

Supplementary data to this article can be found online at https://doi.org/10.1016/j.synbio.2024.01.002.

References

[1] Keerthi M, Boopathy G, Chen SM, Chen TW, Lou BS. A core-shell molybdenum nanoparticles entrapped f-MWCNTs hybrid nanostructured material based non-enzymatic biosensor for electrochemical detection of dopamine neurotransmitter in biological samples. Sci Rep 2019;9(1):13075. https://doi.org/10.1038/s41598-019-48999-0.

[2] Kim DS, Kang ES, Baek S, Choo SS, Chung YH, Lee D, et al. Electrochemical detection of dopamine using periodic cylindrical gold nanoelectrode arrays. Sci Rep 2018;8(1):14049. https://doi.org/10.1038/s41598-018-32477-0.

[3] de Almeida GRL, Szczepanik JC, Selhorst I, Schmitz AE, Dos Santos B, Cunha MP, et al. Methylglyoxal-mediated dopamine depletion, working memory deficit, and depression-like behavior are prevented by a dopamine/noradrenaline reuptake inhibitor. Mol Neurobiol 2021;58(2):735–49. https://doi.org/10.1007/s12035-020-02146-3.

[4] Turk AZ, Lotfi Marchoubeh M, Fritsch I, Maguire GA, SheikhBahaei S. Dopamine, vocalization, and astrocytes. Brain Lang 2021;219:104970. https://doi.org/10.1016/j.bandl.2021.104970.

[5] Lan GP, Jiao CJ, Wang GQ, Sun YH, Sun Y. Effects of dopamine on growth, carbon metabolism, and nitrogen metabolism in cucumber under nitrate stress. SCI HORTIC-AMSTERDAM 2020;260:108790. https://doi.org/10.1016/j.scienta.2019.108790.

[6] Gao T, Zhang Z, Liu X, Wu Q, Chen Q, Liu Q, et al. Physiological and transcriptome analyses of the effects of exogenous dopamine on drought tolerance in apple. Plant Physiol Biochem 2020;148:260–72. https://doi.org/10.1016/j.plaphy.2020.01.022.

[7] Gao S, Ma D, Wang Y, Zhang A, Wang X, Chen K. Whole-cell catalyze L-dopa to dopamine via co-expression of transport protein AroP in *Escherichia coli*. BMC Biotechnol 2023;23(1):33. https://doi.org/10.1186/s12896-023-00794-6.

[8] Shishov VA, Kirovskaia TA, Kudrin VS, Oleskin AV. Amine neuromediators, their precursors, and oxidation products in the culture of *Escherichia coli* K-12. Prikl Biokhim Mikrobiol 2009;45(5):550–4. https://doi.org/10.1134/S0003683809050068.

[9] Villageliú D, Lyte M. Dopamine production in *Enterococcus faecium*: a microbial endocrinology-based mechanism for the selection of probiotics based on neurochemical-producing potential. PLoS One 2018;13(11):e0207038. https://doi.org/10.1371/journal.pone.0207038.

[10] Yang T, Wu P, Zhang Y, Cao M, Yuan J. High-titre production of aromatic amines in metabolically engineered *Escherichia coli*. J Appl Microbiol 2022;133(5):2931–40. https://doi.org/10.1111/jam.15745.

[11] Jiao X, Li Y, Zhang X, Liu C, Liang W, Li C, et al. Exogenous dopamine application promotes alkali tolerance of apple seedlings. Plants 2019;8(12):580. https://doi.org/10.3390/plants8120580.

[12] Li C, Sun XK, Chang C, Jia DF, Wei ZW, Li CY, et al. Dopamine alleviates salt-induced stress in Malus hupehensis. Physiol Plantarum 2015;153(4):584–602. https://doi.org/10.1111/ppl.12264.

[13] Liang B, Gao T, Zhao Q, Ma C, Chen Q, Wei Z, et al. Effects of exogenous dopamine on the uptake, transport, and resorption of apple ionome under moderate drought. Front Plant Sci 2018;9:755. https://doi.org/10.3389/fpls.2018.00755.

[14] Ahmad A, Khan WU, Shah AA, Yasin NA, Ali A, Rizwan M, et al. Dopamine alleviates hydrocarbon stress in Brassica oleracea through modulation of physio-biochemical attributes and antioxidant defense systems. Chemosphere 2021;270:128633. https://doi.org/10.1016/j.chemosphere.2020.128633.

[15] Mo X, Cai X, Hui Q, Sun H, Yu R, Bu R, et al. Whole genome sequencing and metabolomics analyses reveal the biosynthesis of nerol in a multi-stress-tolerant *Meyerozyma guilliermondii* GXDK6. Microb Cell Factories 2021;20(1):4. https://doi.org/10.1186/s12934-020-01490-2.

[16] Villa-Rodríguez E, Ibarra-Gámez C, de Los Santos-Villalobos S. Extraction of high-quality RNA from *Bacillus subtilis* with a lysozyme pre-treatment followed by the Trizol method. J Microbiol Methods 2018;147:14–6. https://doi.org/10.1016/j.mimet.2018.02.011.

[17] Zhai Y, Liu X, Huang Z, Zhang J, Stalin A, Tan Y, et al. Data mining combines bioinformatics discover immunoinfiltration-related gene SERPINE1 as a biomarker for diagnosis and prognosis of stomach adenocarcinoma. Sci Rep 2023;13(1):1373. https://doi.org/10.1038/s41598-023-28234-7.

[18] De la Cruz G, Blas R, Pérez W, Neyra E, Ortiz R. Foliar transcriptomes reveal candidate genes for late blight resistance in cultivars of diploid potato *Solanum tuberosum* L. Andigenum Group. Front Plant Sci 2023;14:1210046. https://doi.org/10.3389/fpls.2023.1210046.

[19] Yin XJ, Hong W, Tian FJ, Li XC. Proteomic analysis of decidua in patients with recurrent pregnancy loss (RPL) reveals mitochondrial oxidative stress dysfunction. Clin Proteonomics 2021;18(1):9. https://doi.org/10.1186/s12014-021-09312-2.

[20] Myers SA, Klaeger S, Satpathy S, Viner R, Choi J, Rogers J, et al. Evaluation of advanced precursor determination for tandem mass tag (TMT)-based quantitative proteomics across instrument platforms. J Proteome Res 2019;18(1):542–7. https://doi.org/10.1021/acs.jproteome.8b00611.
[21] Sun H, Cai X, Yan B, Bai H, Meng D, Mo X, et al. Multi-omics analysis of lipid metabolism for a marine probiotic *Meyerozyma guilliermondii* GXDK6 under high NaCl stress. Front Genet 2022;12:798535. https://doi.org/10.3389/fgene.2021.798535.
[22] Pautova AK, Sobolev PD, Revelsky AI. Analysis of phenylcarboxylic acid-type microbial metabolites by microextraction by packed sorbent from blood serum followed by GC-MS detection. Clin Mass Spectrom 2019;14 Pt A:46–53. https://doi.org/10.1016/j.clinms.2019.05.005.
[23] Cai X, Sun H, Yan B, Bai H, Zhou X, Shen P, et al. Salt stress perception and metabolic regulation network analysis of a marine probiotic *Meyerozyma guilliermondii* GXDK6. Front Microbiol 2023;14:1193352. https://doi.org/10.3389/fmicb.2023.1193352.
[24] Ashkenazy H, Abadi S, Martz E, Chay O, Mayrose I, Pupko T, et al. ConSurf 2016: an improved methodology to estimate and visualize evolutionary conservation in macromolecules. Nucleic Acids Res 2016;44(W1):W344–50. https://doi.org/10.1093/nar/gkw408.
[25] Tasinov O, Kiselova-Kaneva Y, Ivanova D, Pasheva M, Vankova D, Ivanova D. *Ferrum phosphoricum* D12 treatment affects J774A.1 cell proliferation, transcription levels of iron metabolism, antioxidant defense, and inflammation-related genes. Homeopathy 2022;111(2):113–20. https://doi.org/10.1055/s-0041-1731312.
[26] Profiti G, Martelli PL, Casadio R. The Bologna Annotation Resource (BAR 3.0): improving protein functional annotation. Nucleic Acids Res 2017;45(W1):W285–90. https://doi.org/10.1093/nar/gkx330.
[27] Su Y, DePasquale M, Liao G, Buchler I, Zhang G, Byers S, et al. Membrane bound catechol-O-methytransferase is the dominant isoform for dopamine metabolism in PC12 cells and rat brain. Eur J Pharmacol 2021;896:173909. https://doi.org/10.1016/j.ejphar.2021.173909.
[28] Zeng J, Spiro S. Finely tuned regulation of the aromatic amine degradation pathway in *Escherichia coli*. J Bacteriol 2013;195(22):5141–50. https://doi.org/10.1128/JB.00837-13.
[29] Saranya G, Sruthi D, Jayakumar KS, Jiby MV, Nair RA, Pillai PP, et al. Polyphenol oxidase (PPO) arm of catecholamine pathway catalyzes the conversion of -tyrosine to -DOPA in Mucuna pruriens (L.) DC var. pruriens: an integrated pathway analysis using field grown and in vitro callus cultures. Plant Physiol Biochem 2021;166:1032–43. https://doi.org/10.1016/j.plaphy.2021.06.053.
[30] Sunnadeniya R, Bean A, Brown M, Akhavan N, Hatlestad G, Gonzalez A, et al. Tyrosine hydroxylation in betalain pigment biosynthesis is performed by cytochrome P450 enzymes in beets (beta vulgaris). PLoS One 2016;11(2):e0149417. https://doi.org/10.1371/journal.pone.0149417.
[31] Szklarczyk D, Kirsch R, Koutrouli M, Nastou K, Mehryary F, Hachilif R, et al. The STRING database in 2023: protein-protein association networks and functional enrichment analyses for any sequenced genome of interest. Nucleic Acids Res 2023;51(D1):D638–46. https://doi.org/10.1093/nar/gkac1000.
[32] Zhao M, Tao Y, Wu X, Xiao Y. One-pot efficient biosynthesis of 4-hydroxyphenylacetic acid and its analogues from lignin-related p -coumaric and ferulic acids. ACS Sustainable Chem Eng 2021;9(18):6400–9. https://doi.org/10.1021/acssuschemeng.1c00993.
[33] Jeong SY, Jin H, Chang JH. Crystal structure of L-aspartate aminotransferase from *Schizosaccharomyces pombe*. PLoS One 2019;14(8):e0221975. https://doi.org/10.1371/journal.pone.0221975.
[34] Sieckmann T, Schley G, Ögel N, Kelterborn S, Boivin FJ, Fähling M, et al. Strikingly conserved gene expression changes of polyamine regulating enzymes among various forms of acute and chronic kidney injury. Kidney Int 2023;104(1):90–107. https://doi.org/10.1016/j.kint.2023.04.005.
[35] Jia J, Liu X, Li L, Lei C, Dong Y, Wu G, et al. Transcriptional and translational relationship in environmental stress: RNAseq and ITRAQ proteomic analysis between sexually reproducing and parthenogenetic females in *Moina micrura*. Front Physiol 2018;9:812. https://doi.org/10.3389/fphys.2018.00812.
[36] Stefi AL, Vassilacopoulou D, Christodoulakis NS. Environmentally stressed summer leaves of the seasonally dimorphic Phlomis fruticosa and the relief through the L-Dopa decarboxylase (DDC). Flora Morphology Distribution Functional Ecology of Plants 2019;251:11–9. https://doi.org/10.1016/j.flora.2018.12.002.
[37] Liu Q, Gao T, Liu W, Liu Y, Zhao Y, Liu Y, et al. Functions of dopamine in plants: a review. Plant Signal Behav 2020;15(12):1827782. https://doi.org/10.1080/15592324.2020.1827782.
[38] Das A, Verma A, Mukherjee KJ. Synthesis of dopamine in *E. coli* using plasmid-based expression system and its marked effect on host growth profiles. Prep Biochem Biotechnol 2017;47(8):754–60. https://doi.org/10.1080/10826068.2017.1320291.
[39] Ramos-Moreno L, Ramos J, Michán C. Overlapping responses between salt and oxidative stress in *Debaryomyces hansenii*. World J Microbiol Biotechnol 2019;35(11):170. https://doi.org/10.1007/s11274-019-2753-3.
[40] Ahammed GJ, Wang Y, Mao Q, Wu M, Yan Y, Ren J, et al. Dopamine alleviates bisphenol A-induced phytotoxicity by enhancing antioxidant and detoxification potential in cucumber. Environ Pollut 2020;259:113957. https://doi.org/10.1016/j.envpol.2020.113957.